Journal of Research in Pharmacy

Research Article

www.jrespharm.com

Preparation and Characterization Studies of Nanofiber and Orodispersable Film Formulations of Enoxolone

Juste BARANAUSKAITE-ORTASÖZ [1] *, Burcu ÜNER [1]

[1] Department of Pharmaceutical Technology, Faculty of Pharmacy, Yeditepe University, Istanbul, Turkey.

* Corresponding Author. E-mail: juste.ortasoz@yeditepe.edu.tr (J.O.); Tel. +90-533-150 89 10.

Received: 28 February 2022 / Revised: 24 May 2022 / Accepted: 24 May 2022

ABSTRACT: Enoxolone is a pentacyclic triterpenoid observed from Glycyrrhiza glabra and it has an antibacterial, antiviral and antifungal effects. However, enoxolone (ENX) has low oral bioavailability due to a first pass metabolism effect in the intestinal tract, poor intestinal permeability. The aim of this study was to develop the PVP based orodispersible films (ODFs) containing ENX by electrospinning and solvent casting methods and to compare in terms of their credibility for orodispersible delivery of ENX through a variety of *in vitro* and physical investigations. Physical properties such as thichness, weight variation, tensile strength, Young's modulus and elongation at break were investigated. Moreover, the *in vitro* release profile of ENX from prepared films were characterized in this study. The morphological structures of the prepared film formulations were examined under scanning electron microscope and the interaction between the ENX, film and PVP were determined by the FTIR spectroscopy.DSC analysis was performed to understand the thermal behavior of formulations and components. The results obtained proved that the electrospinning process can be used to produce ODF formulations with lower disintegration time (≈4.52 min), lower diameter (≈218.5 nm) and acceptable mechanical strength (≈370.55 MPa). The preliminary results as a proof-of-concept demonstration reported here will shed a new light on the future design and application of ODFs by electrospinning method.

KEYWORDS: nanofiber, enoxolone, edible film, electrospinning

1. INTRODUCTION

Many recent research is focued on benefits of natural products for human health. Natural compounds and their extracted purified biologically active compounds demostrate varous pharmacological effects, such as antifungal, antibacterial an antioxdant activity [1]. Enoxolone also known as glycyrrhetinic acid (GA) is a pentacyclic triterpenoid extracted from *Glycyrrhiza glabra* which has an antibacterial, antiviral, and antifungal effects [2,3]. Recent studies have proved that enoxolone is able to carboxylate the DNA replication ans inhibit producing microbial toxins and enzymes [4]. However, the high hydrophobicity and low bioavailability of this compound limits the pharmacological effect [5]. The limitations can be controlled by nanocarriers using different kind of polymers [6].

Drugs can be administred in various administration routes, but due to ease of administration and high patient compliance the most common one is the oral route. On the other hand, the oral route has some disadvantages such as dysphagia, lower bioavailability, long onset time and it is not suitable for geriatric, pediatric patients and who has a difficulty to swallow. Nowadays is increasing intrest to produce of new delivery systems to diminish these current disadvantages of orally administrated drugs. Fast-dissolving delivery systems are rapidly gaining interest in the pharmaceutical industry. Moreover, the consumers' interst in the fast-dissolving film has increased recently, due to the advantageus properties of these dosage forms such as rapid disintegration and enhanced dissolution rate, self-administration. Recently, the different kind of the bioadhesive mucosal dosage forms have been produced including, adhesive tablets, gels and polymeric films that is also known as mouth dissolving films [7,8].

How to cite this article: Baranauskaite-Ortasöz J, Üner B, Preparation and Characterization Studies of Nanofiber and Orodispersable Film Formulations of Enoxolone. J Res Pharm. 2022; 26(5): 1242-1251

ISSN: 2630-6344

http://dx.doi.org/10.29228/jrp.216

The main advantages of fast dissolving drug delivery systems are disintegrated or dissolved within a minute, simply placed on the patient's mucosal tissue or tongue. Furhermore, these dosage forms offer specific advantages, including ease of transport, accurate dosing, acceptable taste, handling and rapid onset of action. The orodispersible films can be produced by several methods such as solvent-casting and electrospining methods [8]. However, thin film produced by solvent-casting method has some drawbacks such as the necessity of using plasticizers, which may be subjected to scrutiny for their enviromental hazards and toxicity also for increasing the cost of the final product [9]. Electrospinning is gained an interested as alternative to solvent casting technique due to several main advantages. The produced amorphous fibrous film has enhanced plasticity and flexibility, without using pasticizers and significantly higher surface areas in comparison to films produced by solvent-casting method [10,11]. Moreover, this method also offers high encapsulation efficiency, as there is no loss of drug during the preparation [12]. There are different kind of polymers could be used for producing the nanofibrous film formulations among it, the polyvinylpyrrolidone (PVP), polycaprolactone and polyvinyl alcohol (PVA) are commonly used. These polymers provide good mechanical properties, stability in the body, good flexibility properties [13]. Moreover, the PVP has proved due to its acceptable level of toxicity and biocompatibility [14].

The objective of this study was to develop the PVP based orodispersible films (ODFs) containing enoxolone (ENX) by electrospinning and solvent casting methods as well as compare in terms of their credibility for orodispersible delivery of ENX through a variety of in vitro and physical investigations. The initial work focused on preparing and characterizing physicomechanical properties such as disintegration, in vitro dissolution, Young's modulus, elongation at the break and tensile strength, thichness, weight variation and morpholocial examination. The interaction between the polymer and ENX was determined by an FTIR method. DSC analysis was performed to understand the thermal behavior of formulations and components.

2. RESULTS AND DISCUSSION

2.1. Viscosity and Thickness

Viscosity measurements of both film and nanofiber (NF) formulations were made before solvent-casting and electrospinning processes. No statistically significant difference was observed between the solutions which viscosity was measured ($p > 0.05$) (Table 1). It has been proven that the data on the obtained viscosities (for both film and) are similar to those of other studies [14,15].

As seen in Table 1, the thickness of film formulations is around 73-74 µm, while the thickness of NF formulations is around 46 µm. Studies show that the thickness of film formulations can be change between 10 - 110 µm [15,16]. In studies with nanofiber formulations, it is seen that this thickness changes as 32.4 - 74.6 µm [17]. There were no significant differences between to unloaded and loaded formulations both of film and nanofiber formulation, it was determined that the film formulations were statistically thicker than the nanofiber formulations ($p<0.05$). It is thought that the reason for this is due to the increase in the attraction force applied by the polymers to each other depending on the electrical field application used during the preparation of nanofiber formulations [18].

2.2. Weight variation

As a result of the weight variation studies performed with the formulations, the appropriate results were obtained with the USP Pharmacopeia (< 10% deviation) [19]. Weight variation values were found to vary between 2.18 and 1.89 mg. There was no statistical difference between formulations ($p > 0.05$).

2.3. In vitro disintegration study

Data obtained from various studies give the disintegration time between 20-60 seconds for film formulations, while this time is between 2-30 seconds for nanofiber formulations [20,21]. The results obtained proved that there is a linear proportionality between the thicknesses of the formulations and the disintegration times [22]. It was determined that film formulations were statistically degraded in a longer time than the NF formulations ($p<0.05$). Both film and nanofiber formulations have been confirmed to break down within the times specified in reference studies.

Table 1. Thickness, weigh variation and disintegration time of films and NFs

Formulations	Weigh variation (mg)	Viscosity (cP)	Thickness (µm)	Disintegration time (sec)
UL-NF	1.89 ± 0.01	21.097 ± 0.911	46.29 ± 2.05	4.19 ± 0.37
L-NF	2.11 ± 0.01	21.135 ± 1.424	47.02 ± 1.49	4.86 ± 0.73
L-F	2.13 ± 0.03	19.503 ± 1.005	74.28 ± 2.27*	17.33 ± 2.04*
UL-F	2.18 ± 0.02	19.218 ± 1.329	73.71 ± 1.18*	16.23 ± 1.16*

* It shows that it is statistically different from the others ($p < 0.05$)
UL-F : Unloaded film formulation
UL-NF : Unloaded nanofiber formulation
L-F : Loaded film formulation
L-NF : Loaded nanofiber formulation

Figure 1 shows that disintegration steps of the NF formulation prepared by the electrospinning method. It was determined that NF passed from the A stage to the C stage in ≈2.8 seconds, and it was proven that the speed of disintegration was evident.

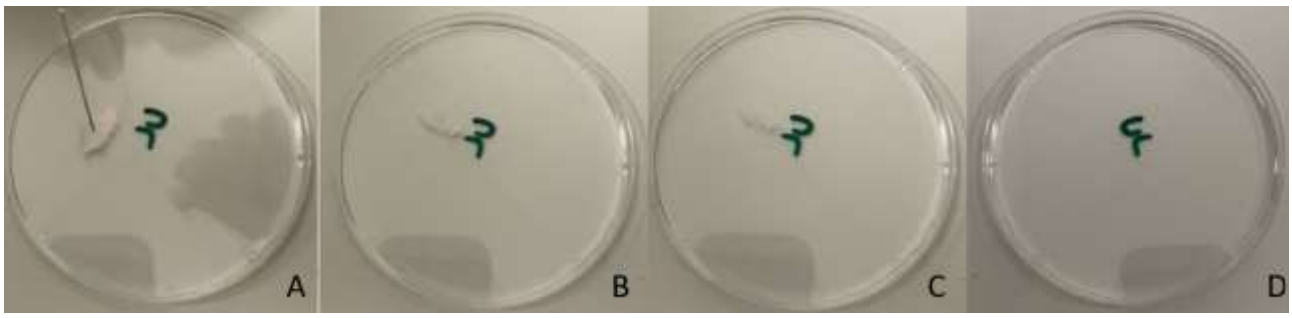

Figure 1. Disintegration steps of NF formulation

2.4. Morphological examination

It has been determined that there is a smooth appearance in general in the SEM images of the film formulations and this appearance is compatible with the reference articles. In the SEM images of the nanofiber formulations, it was observed that the results were compatible with the reference articles prepared using PVP [23,24], while the mean diameters of the UL-NF and L-NF formulations were found to be 216.3 ± 12.3 and 221 ± 9.5 nm, respectively. It was concluded that there was no statistically significant difference between the diameters of the UL-NF and L-NF formulations ($p > 0.05$).

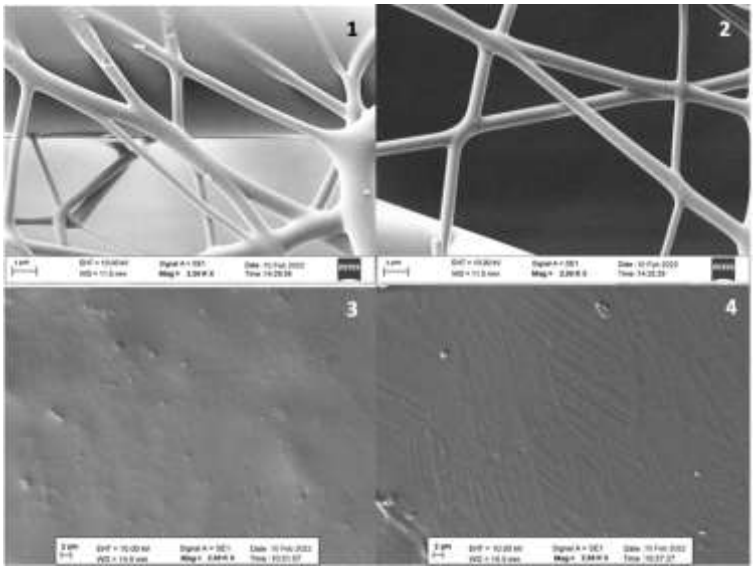

Figure 2. SEM images of film and NF formulations (1: UL-NF, 2: L-NF, 3: UL-F and 4: L-F)

2.5. Texture Properties

For film and NF formulations, the tensile force and Young's modulus were calculated as a result of the texture profile (Table 2). The fact that the tensile strength of the film formulations is higher than that of the NF formulations indicates that they are more rigid [25]. These values are also compatible with the disintegration times. In addition, Young's modulus also increases with the increase in fragility value [26]. The fact that the increase in brittleness value is statistically higher in film formulations than in NF formulations ($p < 0.05$) proves that the elasticity of film formulations is lower than NF formulations. In addition to all this information, when the same type of formulations (Unloaded and loaded) was compared in terms of texture properties, it was determined that there was no statistical difference ($p > 0.05$).

Table 2. Texture profiles of films and NFs

Formulations	Tensile Strength (MPa)	Young's Modulus (MPa)
UL-F	56.29 ± 1.18*	1329.25 ± 33.09*
UL-NF	12.95 ± 2.15	357.39 ± 7.51
L-F	54.35 ± 13.16*	1285.04 ± 27.43*
L-NF	12.28 ± 1.04	383.71 ± 8.13

* It shows that it is statistically different from the others ($p < 0.05$)
UL-F : Unloaded film formulation
UL-NF : Unloaded nanofiber formulation
L-F : Loaded film formulation
L-NF : Loaded nanofiber formulation

2.6. Thermal behaviour

DSC analysis was performed to understand the thermal behavior of formulations and components. It was observed that enoxolone gave a single endothermic peak at 296.54 °C, as determined from the reference articles [27]. As stated in the studies performed with PVP, it was observed a thermogram with 2 endothermic peaks between 150-170 °C (mean 159.2 °C). Glycerol proved to have no crystalline or amorphous formations, resulting in a smooth thermogram. Another remarkable point was that the addition of glycerol caused a statistically significant decrease in melting temperature compared to PVP ($p < 0.05$). The melting temperatures of the UL-F and UL-NF formulations were determined as 133.25 °C and 138.72 °C, respectively. It can be said that the reason for this is demonstrated by the lower melting behavior of the formulation by stretching the covalent bonds with the addition of added glycerol [28].

Finally, a statistically significant increase in melting degrees were observed with the addition of enoxolone compared to formulations without drug load ($p < 0.05$). Melting degrees of L-F and L-NF formulations were determined as 161.33°C and 165.49°C, respectively; it was determined that there was no

statistical difference among them ($p > 0.05$). The reason why increases the melting temperature of enoxolone loaded formulations is thought to be due to the fact that crystallized molecules remain in the formulation due to its rigid structure [29]. In addition, the endothermic peak observed at 296.54°C for enoxolone disappeared in all drug-loaded formulations (L-F and L-NF), which is evidence of complete amorphization of the drug in film formulations.

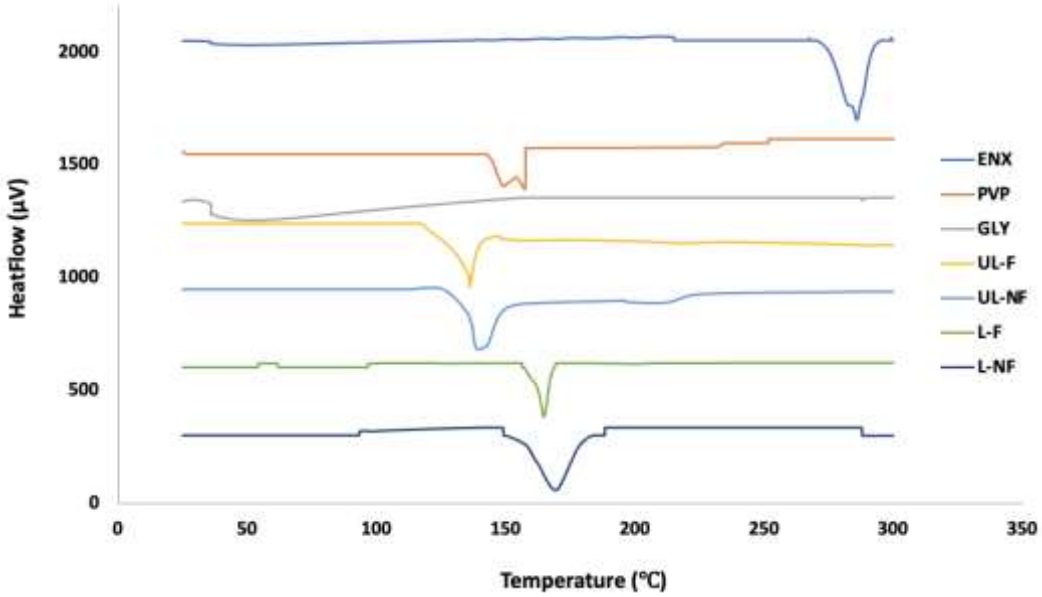

Figure 3. DSC Thermogram of films, NFs and components (ENX: Enoxolone, GLY: Glycerol)

2.7. Fourier Transform-Infrared (FT-IR) Analysis

In the FTIR analysis performed by operating in transmission mode, the specific vibrations of the -COOH group of enoxolone are observed in the 1733 cm^{-1} band in pure enoxolone [30]; It was determined that in L-F and L-NF formulations, these spectra shifted to 1791 cm^{-1} and 1803 cm^{-1} bands. It has been noted that vibrational bands originating from the aliphatic -OH group, which is specific to glycerol, are seen between 2800-2600 cm^{-1} and UL-F and L-F formulations give spectra in this band range. These values have been proven to be compatible with similar studies [31,32].

It has been determined that vibrational bands belonging to the aromatic C-N group specific to PVP are seen at 1302 cm^{-1} and this is consistent with similar studies [33,34]. In all formulations which containing PVP, bands belonging to this group shifted to 1411 cm^{-1}, 1432 cm^{-1}, 1428 cm^{-1} and 1446 cm^{-1} for UL-F, UL-NF, LF and L-NF formulations, respectively.

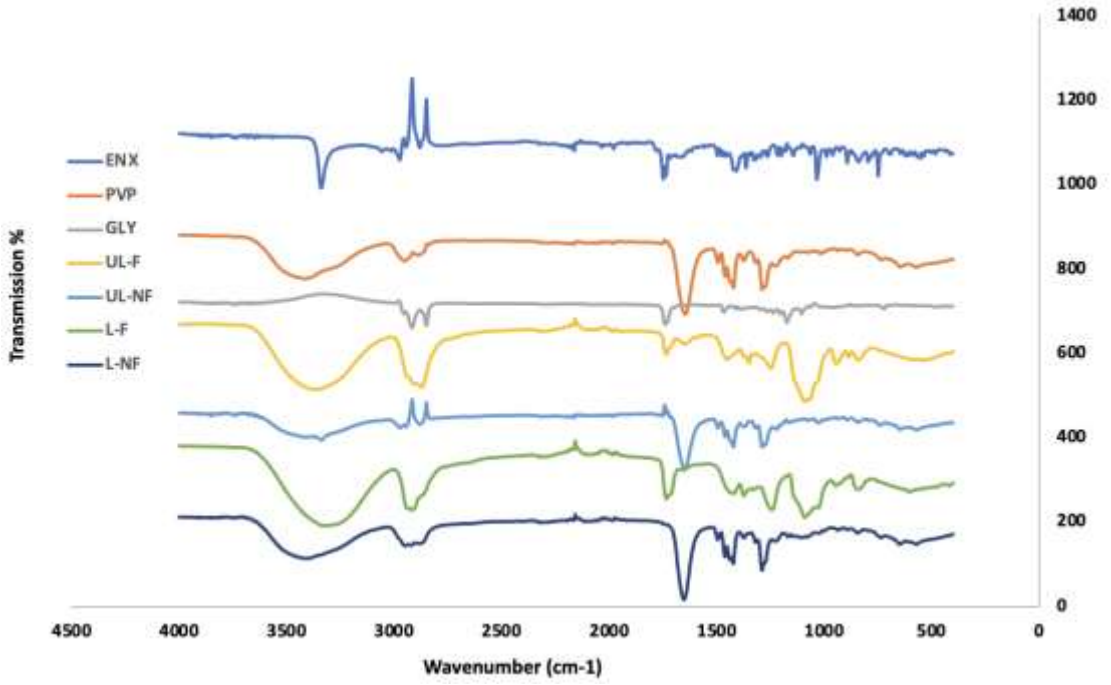

Figure 4. FTIR spectrum formulations and ingredients (ENX: Enoxolone, GLY: Glycerol)

2.7. In vitro dissolution study

The dissolution profile of a dosage form is a crucial for predicting the *in vivo* action of an active pharmaceutical agent. The dissolution profile of L-F and L-NF formulations films (the size of the film was 2 × 2 cm^2 and one film mass was 1.2 g) was shown in Fig. 5. The concentrations were determined by extrapolation of the calibration curve and the graph of present release over time was plotted. Formulation L-NF exhibited the highest initial burst release of about 96.9% within 1 minute. All formulations released entire drug up to the 8 th min ($p < 0.05$). In Figure 5, it was seen that the initial rapid release of the formulations was due to the explosion effect due to elution from the outer surface of the film matrix. It can be said that the reason why this effect creates a statistically significant difference in L-NF formulations is due to the fact that it disintegrates faster than L-F formulations. *In vitro* release studies indicated that the main mechanism of drug release was diffusion as specified in the Fick's first law. The electro spun inclusion complex naofibrous mats have essential properties for enhancing the dissolution and release of poorly soluble active compounds [35]. The burst release of ENX could be ascribed to the following unique properties of the system such as the high-water solubility of the polymer matrix, that promotes the rapid dissolution of nano fibrous matrix and the high surface area, porous and the 3D continuous structure of nano fibrous mats which increase the number of contact sides and the penetration ways for the dissolution medium [35].

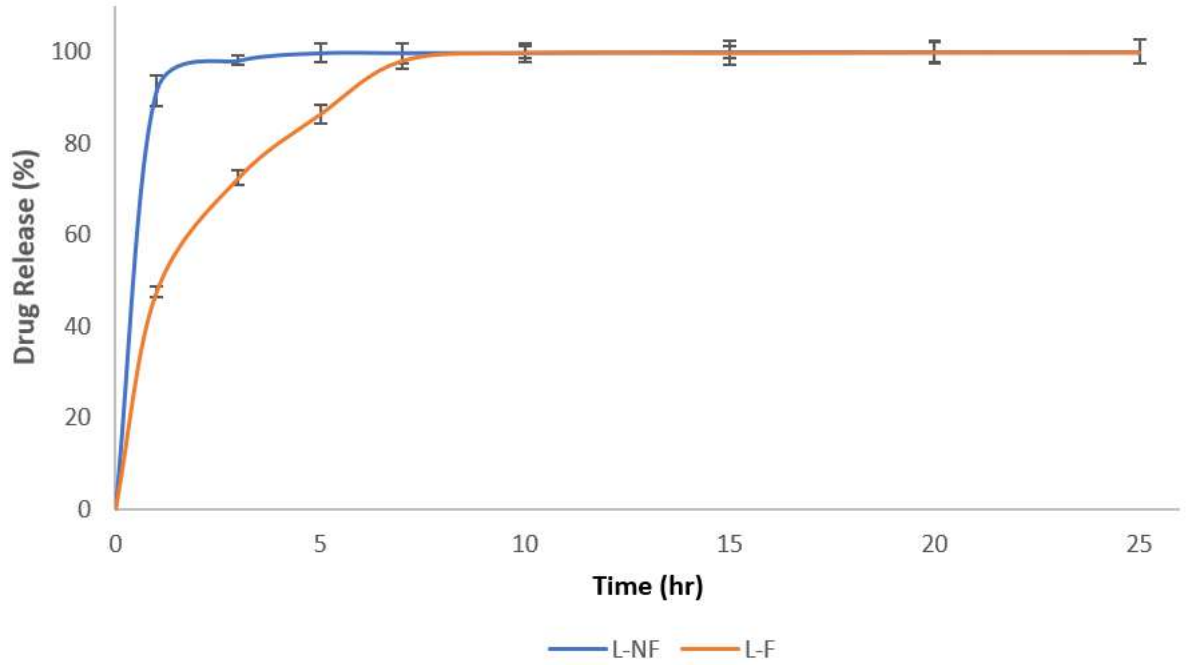

Figure 5. Films and NFs *in vitro* dissolution study

The release versus time profiles from L-F and L-NF formulations were shape-fitted against Zero-order, First-order, Higuchi, Hixson-Crowell and Korsmeyer-Peppas models (Table 3). The correlation was ideally reflected by First-order model. First-order results signified the independence of rate versus the concentrations of ENX along each side of the membrane. According to other research these findings more often reflect a pseudo first-order model, in which dissolution rates could be concentration-dependent [36].

Table 3. Kinetic models of formulation

Formulations	Zero-order (r^2)	First-order (r^2)	Higuchi (r^2)	Hixson-Crowell (r^2)	Korsmeyer-Peppas (r^2, (n))
L-F	0.7879	0.9713*	0.8056	0.7936	0.8339 (0.1655)
L-NF	0.7391	0.9441*	0.8219	0.7164	0.7798 (0.3441)

* It shows that it is statistically different from the others ($p < 0.05$)
L-F : Loaded film formulation
L-NF : Loaded nanofiber formulation

3. CONCLUSION

In this study, ENX loaded ODFs formulations were successfully fabricated using PVP with electro-spinning and solvent casting techniques. Film and NF formulations were compared in terms of mechanical strength, release profile and morphology. It was determined that the film formulations produced by solvent-casting method were statistically thicker than the nanofibrous film formulations. Moreover, it was determined that the film formulations were statistically degraded in a longer time than the NF formulations. The results obtained proved that there is a linear proportionality between the thicknesses of the formulations and the disintegration times. It was determined that there was no statistical difference between the weights of the film and NF formulations. The ODF formulations produced by electro-spinning method promoted reduction of the tensile strength and Young's modulus, and an increase in elongation. The higher dissolution rate within 1 minute was achieved from L-NF formulation. The preliminary results as a proof-of-concept demonstration reported here will shed new light on the future design and application of ODFs by electrospinning method.

4. MATERIALS AND METHODS

4.1. Materials

Enoxolone (>99.5% purity) was provided from Nanjing Seef Biotechnology, China. Polyvinylpyrrolidone (PVP, 360.000 MW) and glycerine were obtained from Sigma Aldrich, Germany. Ethanol was purchased from SDS Chemicals, USA.

4.2. Preparation of formulations

4.2.1. Preparation of Films

The film formulation composed of PVP (20%) and glycerol (1%). In the formulation prepared using solvent casting method, the first stage was completed by dissolving PVP in ethanol and mixing at 400 rpm, 50°C for 1 hour. After adding glycerol to the polymer solution, the blank film formulations were poured into a 6 cm petri dish and incubated at 40°C for 1 day [10,11]. During the preparation of drug-loaded formulations, ENX (1%) was dissolved in ethanol at 400 rpm and 50°C, and then PVP and glycerol were added. After that, the same procedure was followed as for the blank formulations. Polymer solutions viscosity was measured at 100 rpm (25°C) with a viscometer (Brookfield DV2, USA) [11].

4.2.2. Preparation of NFs

For the preparation of NF formulations, firstly, PVP (20%) was dissolved in ethanol, and then the solution was stirred at 400 rpm at 40°C for 4 hours (to prevent bubble formation) (prepared by adding 1% ENX in drug-loaded formulations). NF formulations were prepared by electrospinning technique of polymer solutions that were kept for one day after preparation [17]. During electrospinning, the injection pump (New Era Pump System, USA) was adjusted to an injection speed of 1.313 mL/hr and the distance of the needle tip to the aluminum panel was set to 15 cm. The voltage of the electrospinning cabinet was determined as 20.2 kV [17,18].

Table 4. Ingredients of film and NF formulations

Formulations	PVP (%)	ENX (%)	GLY (%)
UL-F	20	-	1
UL-NF	20	-	-
L-F	20	1	1
L-NF	20	1	-

ENX: Enoxolone
GLY: Glycerol
PVP: Polyvinylpyrrolidone

4.3. Thickness

The thickness (1 cm^2) of the film and nanofiber formulations was measured use to digital caliper (Mitutuyo, Japan). Each measurement was taken from 5 different points belonging to the film and NF formulations [17].

4.4. Weight variation

In the weight deviation measurement of both film and NF formulations, 4 cm^2 samples were cut from 5 different places of the formulations. The weight of each cut sample was determined and the weight deviation was calculated [19].

4.5. In vitro disintegration study

The disintegration study of the prepared film and nanofiber formulations was carried out by modifying the reference studies [21,22]. 10 mL of artificial saliva was added into a 12 cm petri dish. After the film and NF cut as 1 cm^2 were added to the petri dishes, the time until the formulations were completely disintegrated was recorded (n=3).

4.6. Morphological examination

The morphological properties and diameters of the film and nanofiber formulations were analyzed by scanning electron microscope (SEM) (Zeiss, EVO 40, USA) at 10 kV. 4 different samples cut as 1 cm x 1 cm from each formulation were placed on the slide and coated with Au using a sputter coater (Leica, Germany). The mean diameter of the nanofiber formulations was determined using the software of the device (SmartSEM® v05.05 , USA).

4.7. Texture properties

A texture profile analyzer (TA-XT Plus, Stable Micro System, UK) was used to evaluate the mechanistic properties of film and NF formulations. The speed of the probe used during the analysis was 30 mm/min and the load calibration was 2 kg [25,26]. Analysis was performed by taking 3 separate samples of 4 cm^2 from each formulation. Young's modulus and tensile strength values were measured using Exponent software (version 6.0.3).

4.8. Thermal behaviours

Differential scanning calorimetry (DSC) analysis was performed using a DSC device (DSC 131, Setaram, France) in order to determine the behavior of the prepared formulations against heat. The samples were weighed between 6 - 8 mg and placed in aluminum pans for analysis. The temperature was increased between 0-300°C at 10°C /min. Nitrogen gas was applied at 20 mL/min for cooling the system.

4.9. FT-IR Analysis

FTIR device (iS50, Nicolet, Thermo Fisher, USA) was used to make sense of the chemical relationship between ODFs and NFs. In the analysis performed using the ATR mode of the device, 1-5 mg of sample was placed on the plate from which UV beam oncame, and the analysis was performed in the spectrum between 400 cm^{-1} - 4000 cm^{-1}.

4.10. In vitro dissolution study

In vitro release study of the prepared formulations was performed using USP aparattus-1 (Pharmatest, Germany). 6 different vessels were rotated at 50 rpm in 900 mL of simulated salivary fluid (Biochemazone®, Canada, pH 6.6) as release medium at 37.5 ± 0.5°C [35]. At the specified sampling intervals (1,3,5,7,10,15 and 25 minutes), 2 mL samples were taken from the release medium and the amount of drug in the release medium was determined using a UV spectroscopy device (Agilent 1100, USA) at 205 nm [27]. During the dissolution study, care was taken to ensure the sink condition (the same amount of buffer solution was added after 2 mL of sample was taken).

4.11. Statistically Analysis

All analytical values obtained were expressed as mean ± standard deviation. Analyzes were performed using a non-parametric method, ANOVA, and GraphPad® (v. 13.2, Prism, USA) software was used. Values with $p < 0.05$ were considered statistically significant.

Author contributions: Concept – J.O., B.Ü.; Design – J.O., B.Ü.; Supervision – J.O., B.Ü.; Resources – J.O., B.Ü.; Literature Search – J.O., B.Ü.; Writing - J.O., B.Ü.; Critical Reviews – J.O., B.Ü.

Conflict of interest statement: The authors declared no conflict of interest.

REFERENCES

[1] Wu YH, Yu DG, Li JJ, Wang Q, Li HP, Li XY. Medicated multiple-component polymeric nanocomposites fabricated using electrospraying. Polym Polym Compos. 2017; 25, 57-62. [CrossRef]

[2] Xie SR, Zhao J, Liu R. Study and expectation of glycyrrhetic acid. J Dalian Univ. 2005; 26: 84-86. [CrossRef]

[3] Jin M, Wu HJ. Advancement on pharmacological action of glycyrrhetic acid. Med Recapitulate. 2009; 15: 1712–1715. [CrossRef]

[4] Salari MH, Sohrabi N, Kadkhoda Z, Khalili MB. Antibacterial effects of enoxolone on periodontopathogenic and capnophilic bacteria isolated from specimens of periodontitis patients. Iran Biomed J. 2003; 7: 39-42. [CrossRef]

[5] Jin L, Dai L, Ji M, Wang H. Mitochondria-targeted triphenylphosphonium conjugated glycyrrhetinic acid derivatives as potent anticancer drugs. Bioorg Chem. 2019; 85: 179-190. [CrossRef]

[6] Alexander A, Patel RJ, Saraf S, Saraf S. Recent expansion of pharmaceutical nanotechnologies and targeting strategies in the field of phytopharmaceuticals for the delivery of herbal extracts and bioactives. J Control Release. 2016; 241: 110–124. [CrossRef]

[7] Homayun B, Lin X, Choi HJ. Challenges and recent progress in oral drug delivery systems for biopharmaceuticals. Pharmaceutics. 2019; 11: 1-29. [CrossRef]

[8] Jani R, Patel D. Hot melt extrusion: An industrially feasible approach for casting orodispersible film. Asian J Pharm Sci. 2015; 10: 292-305. [CrossRef]

[9] Ghosal K, Chandra A, Roy S, Agatemor C, Thomas S, Provaznik I. Electrospinning over solvent casting: tuning of mechanical properties of membranes. Sci Rep. 2018; 8: 1-9. [CrossRef]

[10] Tian Y, Orlu M, Woerdenbag HJ, Scarpa M, Kiefer O, Kottke D, Sjöholm E, Öblom H, Sandler N, Hinrichs WLJ. Oromucosal films: From patient centricity to production by printing techniques. Expert Opin Drug Deliv. 2019; 16: 981–993. [CrossRef]

[11] Chachlioutaki K, Tzimtzimis EK, Tzetzis D, Chang MW, Ahmad Z, Karavasili C, Fatouros DG. Electrospun Orodispersible Films of Isoniazid for Pediatric Tuberculosis Treatment. Pharmaceutics. 2020; 12: 1-14. [CrossRef]

[12] Zhang H, Niu Q, Wang N, Nie J, Ma G. Thermo-sensitive drug controlled release PLA core/PNIPAM shell fibers fabricated using a combination of electrospinning and UV photo-polymerization. Eur Polym J. 2015; 71: 440–450. [CrossRef]

[13] Li C, Yu DG, Williams GR, Wang ZH. Fast-dissolving core-shell composite microparticles of quercetin fabricated using a coaxial electrospray process. PLoS ONE. 2014; 9: 1-9. [CrossRef]

[14] Vongsetskul T, Wongsomboon TCP, Rangkupan R. Effect of solvent and processing parameters on electrospun polyvinylpyrrolidone ultra-fine fibers. Chiang Mai J Sci. 2015; 42: 436-442. [CrossRef]

[15] Preis M, Pein M, Breitkreutz J. Development of a taste-masked orodispersible film containing dimenhydrinate. Pharmaceutics. 2012; 4(4): 551-562. [CrossRef]

[16] Takeuchi Y, Umemura K, Tahara K, Takeuchi H. Formulation design of hydroxypropyl cellulose films for use as orally disintegrating dosage forms. J Drug Deliv Sci Technol. 2018; 46: 93-100. [CrossRef]

[17] Molla S, Compan V. Polyvinyl alcohol nanofiber reinforced Nafion membranes for fuel cell applications. J Membr Sci. 2011; 372(1-2): 191-200. [CrossRef]

[18] Zhao K, Wang W, Teng A, Zhang K, Ma Y, Duan S, Guo Y. Using cellulose nanofibers to reinforce polysaccharide films: Blending vs layer-by-layer casting. Carbohydr Polym. 2020; 227: 1-9. [CrossRef]

[19] Mushtaque M, Muhammad IN, Hassan SMF, Ali A, Masood R. Development and pharmaceutical evaluation of oral fast dissolving thin film of escitalopram: A patient friendly dosage form. Pak J Pharm Sci. 2020; 33(1): 183-189. [CrossRef]

[20] Yu DG, Branford-White C, White K. Dissolution Improvement of Electrospun Nanofiber-Based Solid Dispersions for Acetaminophen. AAPS PharmSciTech. 2010; 11: 809–817. [CrossRef]

[21] Nagaraju T, Gowthami R, Rajashekar M, Sandeep S, Mallesham M, Sathish D, Shravan Kumar Y. Comprehensive review on oral disintegrating films. Curr Drug Deliv. 2013; 10(1): 96-108. [CrossRef]

[22] Garsuch V, Breitkreutz J. Comparative investigations on different polymers for the preparation of fast-dissolving oral films. J Pharm Pharmacol. 2010; 62(4): 539-545. [CrossRef]

[23] Tong Y, Jiang Z, Wang C, Xin Y, Huang Z, Liu S, Li C. Effect of annealing on the morphology and properties of ZnS: Mn nanoparticles/PVP nanofibers. Mater Lett. 2008; 62(19): 3385-3387. [CrossRef]

[24] Chamakh M, Ayesh AI. Production and investigation of flexible nanofibers of sPEEK/PVP loaded with RuO2 nanoparticles. Mater Des. 2021; 204: 1-8. [CrossRef]

[25] Yang B, Wang L, Zhang M, Luo J, Ding X. Timesaving, high-efficiency approaches to fabricate aramid nanofibers. ACS nano. 2019; 13(7): 7886-7897. [CrossRef]

[26] Galdeano MC, Mali S, Grossmann MVE, Yamashita F, García MA. Effects of plasticizers on the properties of oat starch films. Mater Sci Eng C. 2009; 29(2): 532-538. [CrossRef]

[27] Dong L, Mai Y, Liu Q, Zhang W, Yang J. Mechanism and improved dissolution of glycyrrhetinic acid solid dispersion by alkalizers. Pharmaceutics. 2020; 12(1): 1-24. [CrossRef]

[28] Ma X, Qiao C, Wang X, Yao J, Xu J. Structural characterization and properties of polyols plasticized chitosan films. Int. J Biol Macromol. 2019; 135: 240-245. [CrossRef]

[29] He X, Yu S, Dong Y. Preparation and properties of a novel thermo-responsive poly(N-isopropylacrylamide) hydrogel containing glycyrrhetinic acid. J Mater Sci. 2009; 44: 4078–4086. [CrossRef]

[30] Zhang C, Liu Z, Zheng Y, Geng Y, Han C, Shi Y, Kong L. Glycyrrhetinic acid functionalized graphene oxide for mitochondria targeting and cancer treatment in vivo. Small. 2018; 14(4): 1-16. [CrossRef]

[31] Ren HM, Cai C, Leng CB, Pang SF, Zhang YH. Nucleation Kinetics in Mixed $NaNO_3$/Glycerol Droplets Investigated with the FTIR–ATR Technique. J Phys Chem. 2016; 120(11): 2913-2920. [CrossRef]

[32] Striugas N, Skvorčinskienė R, Paulauskas R, Zakarauskas K, Vorotinskienė L. Evaluation of straw with absorbed glycerol thermal degradation during pyrolysis and combustion by TG-FTIR and TG-GC/MS. Fuel. 2017; 204: 227-235. [CrossRef]

[33] Borodko Y, Habas SE, Koebel M, Yang P, Frei H, Somorjai GA. Probing the Interaction of Poly (vinylpyrrolidone) with Platinum Nanocrystals by UV− Raman and FTIR. *J* Phys Chem. 2006; 110(46): 23052-23059. [CrossRef]

[34] Abdelghany AM, Mekhail MS, Abdelrazek EM, Aboud MM. Combined DFT/FTIR structural studies of monodispersed PVP/Gold and silver nano particles. J Alloys Compd. 2015; 646: 326-332. [CrossRef]

[35] Celebioglu A, Uyar T. Metronidazole/Hydroxypropyl-β-Cyclodextrin inclusion complex nanofibrous webs as fast-dissolving oral drug delivery system. Int J Pharm. 2019; 572: 1-36. [CrossRef]

[36] Baranauskaite J, Adomavičiūtė E, Jankauskaitė V, Marksa M, Barsteigienė Z, Bernatoniene J. Formation and investigation of electrospun Eudragit E100/oregano mats. Molecules. 2019; 24: 1-13. [CrossRef]